JOURNAL OF COMPUTATIONAL PHYSICS 93, 376–387 (1991)

Treatment of Angular Derivatives in the Schrödinger Equation by the Finite Fourier Series Method

R. P. RATOWSKY AND J. A. FLECK, JR.

Lawrence Livermore National Laboratory, Livermore, California 94550

Received September 6, 1989; revised February 8, 1990

We describe a finite Fourier series method for treating the angular derivatives in the angular momentum term of the time-dependent Schrödinger equation in spherical coordinates. The method involves a power series expansion of the evolution operator and treatment of singularities at $\theta = 0$ by L'Hospital's rule. It is demonstrated that the method is accurate across the entire spectrum of the angular momentum operator for an appropriate sampling grid.

1. INTRODUCTION

Considerable progress has been made in solving the time-dependent Schrödinger equation numerically in terms of finite Fourier series, implemented through use of the FFT algorithm [1–7]. One of these methods [1–2] combines operator splitting with a finite Fourier series representation of the wave function. This method is easiest to apply in Cartesian coordinates, where a simple symmetrized operator split affords second-order accuracy with respect to commutation errors, while maintaining the unitarity of the evolution operator.

If one is working in spherical polar coordinates a more complicated operator splitting is required [3] due to the presence of three noncommuting operators in the Hamiltonian, namely, the kinetic energy, the angular momentum, and the potential energy terms. One way to treat the angular momentum factor in the evolution operator split is to express the angular dependence of the wave function in terms of spherical harmonics. One disadvantage of using spherical harmonics as a basis set is that a transformation between the angular momentum values and the sampled angles does not exist with numerical efficiency comparable to that of the FFT relationship between sampled momenta and coordinates. This makes computational running time go up as L^2, rather than $L \ln L$, which would be the case for an FFT transformation, where L is the maximum number of angular momentum basis states involved in the calculation. In this article we describe a method for implementing a solution to the Schrödinger equation in polar coordinates, by use of a finite Fourier series in the polar angle, which is both accurate and efficient and has the added appeal of simplicity.

0021-9991/91 $3.00

Recently a simple but accurate method has been reported [8] for solving the paraxial wave equation in cylindrical polar coordinates in terms of a finite Fourier series. The method is based on a fourth-order Taylor series expansion of the evolution operator with derivatives evaluated by term by term differentiation of a finite Fourier series. Terms that are singular at $r=0$ are treated by applying L'Hospital's rule. Although the Taylor series algorithm is not formally unitary, deviations of the field norm from the initial value are insignificant as long as axial propagation steps are small enough to maintain stability and accuracy of the solution. This method avoids altogether the difficulties associated with the numerical application of Fourier–Bessel transforms [9].

In this article we show that the same procedure is applicable to the angular momentum term in the Schrödinger equation in polar coordinates. The method that we discuss here can be easily generalized to other curvilinear coordinate systems and should greatly facilitate wave-packet analysis in higher dimensional problems.

2. Schrödinger Equation in Spherical Polar Coordinates

The Schrödinger equation in spherical polar coordinates can be written in atomic units as

$$i\frac{\partial \Phi}{\partial t} = H\Phi, \tag{1}$$

where $\Phi = r\Psi$ is the reduced wave function and

$$\begin{aligned} H &= \frac{1}{2\mu}\frac{\partial^2}{\partial r^2} + \frac{L^2}{2\mu r^2} + V(r,\theta) \\ L^2 &= -\frac{1}{\sin\theta}\frac{\partial}{\partial\theta}\left(\sin\theta\frac{\partial}{\partial\theta}\right) + \frac{m^2}{\sin^2\theta}. \end{aligned} \tag{2}$$

We wish to find a solution to Eq. (2) in the form of a two-dimensional Fourier series in r and θ,

$$\Phi(r,\theta) = \sum_{m=-M/2+1}^{M/2} \sum_{n=-N/2+1}^{N/2} \Phi_{mn} \exp\{i[\pi m r/R_0 + n\theta]\}. \tag{3}$$

In its r-dependence $\Phi(r,\theta)$ is continued from positive to negative values of r. The r-dependence has already been discussed in Ref. [3] and will not be considered further here. Instead we focus our attention on the θ-dependence. If we suppress the

radial derivatives from the Hamiltonian in Eq. (2), the Schrödinger equation becomes

$$i\frac{\partial \Phi}{\partial t} = -\frac{1}{2I}\left[\frac{1}{\sin\theta}\frac{\partial}{\partial\theta}\left(\sin\theta\frac{\partial\Phi}{\partial\theta}\right) - \frac{m^2}{\sin^2\theta}\Phi\right] + V(\theta)\Phi$$

$$= -\frac{1}{2I}\left[\frac{\partial^2\Phi}{\partial\theta^2} + \cot\theta\frac{\partial\Phi}{\partial\theta} - \frac{m^2}{\sin^2\theta}\Phi\right] + V(\theta)\Phi, \tag{4}$$

where $I = \mu r^2$ is the moment of inertia.

We shall look for a solution to Eq. (4) in the band-limited Fourier series form, valid on the interval $-\pi \leqslant \theta < \pi$,

$$\Phi(\theta) = \sum_{n=-N/2+1}^{N/2} \Phi_n e^{in\theta}. \tag{5}$$

In general, the evaluation of the coefficients in Eq. (5) by an FFT will require N sampling points, and the finite Fourier series in Eq. (5) will be an exact representation for any function that can be represented as a sum of associated Legendre functions up to and including order $N/2$, i.e., for

$$\Phi(\theta) = \sum_{n=0}^{N/2-1} a_n^m P_n^m(\cos\theta). \tag{6}$$

This follows from the fact that P_n^m can be expressed as

$$P_n^m(\cos\theta) = \sum_{n'=0}^{n} a_{n'}^m \cos n'\theta, \qquad \text{for} \quad m \text{ even};$$

$$P_n^m(\cos\theta) = \sum_{n'=0}^{n} b_{n'}^m \sin n'\theta, \qquad \text{for} \quad m \text{ odd}. \tag{7}$$

If Eq. (4) is written as

$$i\frac{\partial\Phi}{\partial t} = H_\theta \Phi, \tag{8}$$

the solution can be expressed formally to fourth order as

$$\Phi(\Delta t) = e^{-iH_\theta \Delta t}\Phi(0)$$

$$= \left\{1 - i\,\Delta t H_\theta - \frac{1}{2}(\Delta t)^2 H_\theta^2 + \frac{i}{6}(\Delta t)^3 H_\theta^3 + \frac{1}{24}(\Delta t)^4 H_\theta^4 + O((\Delta t)^5)\right\}\Phi(0). \tag{9}$$

The use of the fourth-order expansion (9) implies that all errors including commutation errors are no greater than fifth order. The split operator method, on the other hand, involves a third-order commutation error.

If we express the solution to Eq. (4) as the band-limited Fourier series (5), the derivatives in Eqs. (4) and (9) can be evaluated by term by term differentiation of Eq. (5) to give

$$\frac{\partial \Phi}{\partial \theta} = \sum_{n=-N/2+1}^{N/2} \Phi_n (in) e^{in\theta}, \tag{10}$$

$$\frac{\partial^2 \Phi}{\partial \theta^2} = \sum_{n=-N/2+1}^{N/2} \Phi_n (in)^2 e^{in\theta}. \tag{11}$$

To evaluate the derivatives in Eqs. (10) and (11) requires one FFT pair for each derivative. Terms on the right-hand side of Eq. (4) that are singular at $\theta = 0$ can be evaluated by L'Hospital's rule to give

$$\lim_{\theta \to 0} \cot \theta \frac{\partial \Phi}{\partial \theta} = \left(\frac{\partial^2 \Phi}{\partial \theta^2} \right)_{\theta = 0}, \tag{12a}$$

$$\lim_{\theta \to 0} \frac{m^2}{\sin^2 \theta} \Phi = \frac{m^2}{2} \left(\frac{\partial^2 \Phi}{\partial \theta^2} \right)_{\theta = 0}. \tag{12b}$$

These values are available from the computed array corresponding to Eq. (11).

The Taylor series (9) is equivalent to a fourth-order Runge–Kutta scheme for a time-independent potential. The present scheme can be generalized to time-dependent potentials if one applies the standard Runge–Kutta scheme as used in the solution of ordinary differential equations [10]. As in the Taylor series method, four separate function evaluations of the right-hand side of Eq. (4) will be required.

Tal-Ezer and Kosloff [11] have developed a scheme, applicable strictly to time independent potentials, whereby the evolution operator is represented by a finite sum of complex Chebychev polynomials. At a cost of some additional storage requirements this scheme represents the optimum polynomial approximation of a given order to the evolution operator. For problems in which one is interested in evolving an initial state to some finite state after a significant elapse of time the Tal-Ezer–Kosloff method is the preferred method because of its superior accuracy and efficiency, measured by the number of required Hamiltonian operations. The Taylor series–Runge–Kutta scheme, on the other hand, represents a simple but accurate scheme to be used for marching a solution to a final state through a sequence of intermediate sampling times, and it is applicable to both time-independent as well as time-dependent potentials with comparable accuracy.

3. Computation of Eigenvalues

Eigenvalues can be computed from wave packet evolution by first computing the correlation function [1]

$$\mathscr{P}(t) = \langle \Phi(0) | \Phi(t) \rangle$$

$$= 2\pi \int_0^{\pi} d\theta \sin\theta \Phi^*(\theta, 0)\, \Phi(\theta, t). \tag{13}$$

Substitution from Eq. (5) into Eq. (13) gives

$$\mathscr{P}(t) = -i\pi \sum_{m=-N/2+1}^{N/2} \sum_{n=-N/2+1}^{N/2} \Phi_m^*(0)\, \Phi_n(t)$$

$$\times \int_0^{\pi} [e^{i(n-m+1)\theta} - e^{i(n-m-1)\theta}]\, d\theta$$

$$= \sum_{m=-N/2+1}^{N/2} \sum_{n=-N/2+1}^{N/2} \Phi_m^*(0)\, \Phi_n(t) a_{mn}, \tag{14}$$

where

$$a_{mn} = \begin{cases} \pi\left(\dfrac{1}{n-m+1} - \dfrac{1}{n-m-1}\right), & n-m \text{ even;} \\ 0, & n-m \text{ odd.} \end{cases} \tag{15}$$

The double summation in Eq. (14) can be reduced to the single summation

$$\mathscr{P}(t) = \sum_{n=-N/2+1}^{N/2} A_n \Phi_n(t), \tag{16}$$

where the coefficients

$$A_n = \sum_{m=-N/2+1}^{N/2} a_{mn} \Phi_m^*(0) \tag{17}$$

are compured once at the beginning of the run. The wave function norm is computed in similar fashion from the following expression:

$$|\langle \Phi(t) | \Phi(t) \rangle|^2 = 2\pi \int_0^{\pi} d\theta \sin\theta \Phi^*(t)\, \Phi(t)$$

$$= \sum_{m=-N/2+1}^{N/2} \sum_{n=-N/2+1}^{N/2} \Phi_m^*(t)\, \Phi_n(t) a_{mn}. \tag{18}$$

Expressions (14) and (18) are exact for the representation (5) and thus avoid the errors that would be incurred by performing the corresponding integrations numerically in direct space.

The energy spectrum corresponding to the initial wave packet is constructed by evaluating numerically the Fourier transform

$$\mathscr{P}(E)=\frac{1}{T}\int_0^T dt\, w(t)\, e^{iEt}\mathscr{P}(t), \tag{19}$$

where $w(t)$ is the Hanning window function,

$$w(t)=1-\cos(2\pi t/T) \qquad \text{if} \quad 0\leqslant t\leqslant T. \tag{20}$$

Equation (19) takes the form

$$\mathscr{P}(E)=\sum_n |a_n|^2\, \mathscr{L}(E-E_n), \tag{21}$$

where $|a_n|^2$ is the weight of the state $|E_n\rangle$ in the initial wave packet, and the line-shape function $\mathscr{L}(E-E_n)$ is defined by

$$\begin{aligned}\mathscr{L}(E-E_n)&\equiv\frac{1}{T}\int_0^T dt e^{i(E-E_n)t}w(t)\\ &=\frac{e^{i(E-E_n)T}-1}{i(E-E_n)}\\ &\quad\times\frac{1}{2i}\left[\frac{e^{i[(E-E_n)T+2\pi]}-1}{(E-E_n)T+2\pi}+\frac{e^{i[(E-E_n)T-2\pi]}-1}{(E-E_n)T-2\pi}\right].\end{aligned} \tag{22}$$

The eigenvalues can be determined to high accuracy from the calculated spectrum (19) using the line-shape fitting technique described in Refs. [1–3].

4. Solution for a Rigid Rotor

To illustrate the method and its accuracy we consider first the Schrödinger equation for a rigid three-dimensional rotor with moment of inertia $I=\frac{1}{2}$. Setting $V(\theta)=0$ in Eq. (4), we obtain

$$\begin{aligned}i\frac{\partial\Phi}{\partial t}&=-\frac{1}{2I}\left[\frac{1}{\sin\theta}\frac{\partial}{\partial\theta}\left(\sin\theta\frac{\partial\Phi}{\partial\theta}\right)-\frac{m^2}{\sin^2\theta}\Phi\right]\\ &=-\frac{1}{2I}\left[\frac{\partial^2\Phi}{\partial\theta^2}+\cot\theta\frac{\partial\Phi}{\partial\theta}-\frac{m^2}{\sin^2\theta}\Phi\right].\end{aligned} \tag{23}$$

As a test of the accuracy of the method, we have computed all eigenvalues for Eq. (23) obtainable from N sampled points. Because the stationary-state eigenfunc-

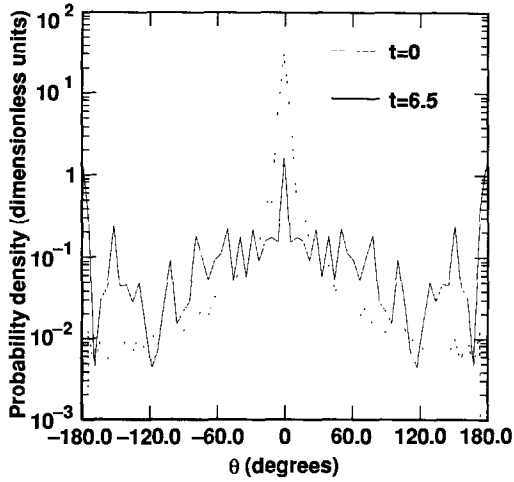

FIG. 1. Wave packets for a rigid rotor. The initial wave packet and the wave packet at $t = 6.5$ superposed.

tions are the Legendre polynomials $P_n(\cos\theta)$, an initial state spanning the full bandwidth allowed by the sampling grid is represented by the linear combination

$$\Phi(\theta, 0) = \sum_{n=0}^{N/2-1} P_n(\cos\theta). \tag{24}$$

We have propagated the initial state (24) using $N = 64$ grid points for 2^{16} steps and a step size $\Delta t = 0.0001$. For this time step the normalization (18) is preserved to

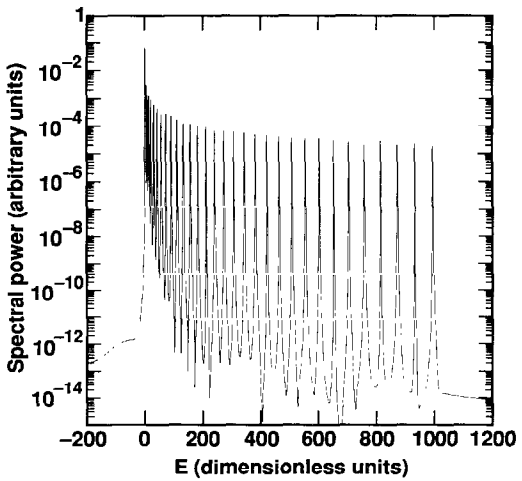

FIG. 2. Bandlimited energy spectrum for a rigid rotor. Angular sampling grid has 64 points. Position of peaks gives seven significant figure accuracy for eigenvalues of the 32 states.

TABLE I

Computed Eigenvalues for the Rigid Rotor Compared with Analytical Values

E (computed)	E (analytical)	l	E (computed)	E (analytical)	l
6.1278667×10^{-9}	0	0	271.9999925	272	16
1.9999993	2	1	306.0000026	306	17
6.0000058	6	2	342.0000074	342	18
12.0000978	12	3	379.9999817	380	19
19.9999573	20	4	419.9999914	420	20
30.0000179	30	5	461.9999853	462	21
41.9999673	42	6	505.9999691	506	22
56.0000327	56	7	551.9999541	552	23
72.0000290	72	8	599.9999461	600	24
89.9999874	90	9	649.9999027	650	25
110.0000119	110	10	701.9998571	702	26
132.0000191	132	11	755.9997851	756	27
155.9999996	156	12	811.9997089	812	28
181.9999952	182	13	869.9995676	870	29
210.0000010	210	14	929.9994230	930	30
240.0000028	240	15	991.9991899	992	31

Note. Parameters are given in the text. All eigenvalues except the first three were generated from a single run using Eq. (24) as the initial condition. The first three were not well isolated in the generated spectrum and were calculated in separate runs.

better than one part in 10^5. No attempt was made, however, to optimize the time step with respect to accuracy and efficiency.

The initial wave packet and the wave packet at the end of the run are superposed in Fig. 1. The initial spike is due to the perfect phasing of all the component states. The dephasing of the state amplitudes results in the spreading of the wave packets at late times.

The energy spectrum of the wave packet is shown in Fig. 2 and the 32 computed eigenvalues are listed and compared with their analytic counterparts, i.e., $l\,(l+1)$, in Table I. It is seen from Table I that eigenvalues are accurate, typically, to seven significant figures. These results demonstrate the accuracy of the method across the entire spectrum of the angular momentum operator.

5. Solution for a Rigid Dipole in a Constant Field

A second application of the method is to a rigid dipole in a constant electric field. For an electric field of magnitude E oriented along the z-axis and a dipole of strength p, $V(\theta)$ takes the form

$$V(\theta) = -pE\cos\theta. \tag{25}$$

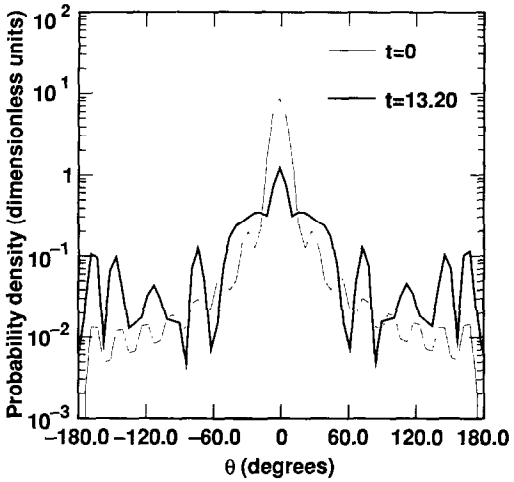

FIG. 3. Wave packets for a rigid rotor in a uniform electric field. The initial wave packet and the wave packet at $t = 13.20$ superposed.

TABLE IIa

Eigenvalues for Rigid Dipole in a Constant Electric Field

E (spectral)	E (variational)	E (perturbation)	l
$-2.36561^{(a)}$	−2.3656		0
2.63875	2.6388		1
6.64546	6.6455		2
12.28624	12.286		3
$20.16352^{(b)}$	20.164		4
30.10714	30.107		5
42.07587	42.076	42.076	6
56.05660	56.057	56.057	7
72.04389		72.044	8
90.0350		90.035	9
110.0287		110.026	10
132.0239		132.024	11
156.0202		156.020	12
182.0173		182.017	13
210.0149		210.015	14
240.0131		240.013	15

Note. Comparison between spectral and variational methods and second-order perturbation theory. The latter two are provided by Ref. [12]. The value l, when it appears, designates the l-value of the unperturbed state. $\omega = 5.0$.

[a] 64 sample points; $\Delta t = 0.0008$; 32K time steps; $\Phi(0) = P_1$.

[b] 64 sample points; $\Delta t = 0.0002$; 64K time steps; $\Phi(0) = P_0 - P_{15}$.

TABLE IIb

Eigenvalues for Rigid Dipole in Constant Electric Field

E (spectral)	E (variational)	E (perturbation)	l
−6.04507[c]	−6.0451		0
7.87936	7.8793		2
13.23939	13.239		3
20.67081	20.671		4
30.43238	30.432		5
42.30473	42.305	42.303	6
56.22715	56.227	56.226	7
72.17577		72.175	8
90.14020		90.140	9
110.11452		110.114	10
132.09551		132.095	11
156.08054		156.081	12
182.06906		182.069	13
210.05984		210.060	14
240.05223		240.052	15

Note. Comparison between spectral and variational methods and second-order perturbation theory. The latter two are provided by Ref. [12]. The value l, when it appears, designates the l-value of the unperturbed state. $\omega = 10.0$.

[c] 64 sample points; $\Delta t = 0.00025$; 64K timesteps; $\Phi(0) = \sum_{n=0}^{15} P_n(\cos\theta)$.

TABLE IIc

Eigenvalues for Rigid Dipole in Constant Electric Field

E (spectral)	E (variational)
−40.50678[d]	−40.507
−21.56488	−21.565
3.77155	3.7716
12.72524	12.725
27.68132	27.681
40.56613	40.566
50.98419	50.984
62.22239	62.223
76.60073	

Note. Comparison between spectral and variational methods. The latter is provided by Ref. [12]. $\omega = 50.0$.

[d] 64 sample points; $\Delta t = 0.0002$; 64 time steps; $\Phi(0) = \sum_{n=0}^{3} P_n(\cos\theta)$.

TABLE IId

Eigenvalues for Rigid Dipole in Constant Electric Field

E (spectral)	E (variational)
$-468.87905^{(e)}$	-468.88
-406.65008	-406.65
-345.45951	-345.46
-285.33526	-285.34
-26.30840	-226.31
-168.41269	-168.41
-111.68619	-111.69
-56.17044	-56.170
-1.91267	
51.03190	
102.60269	
152.72730	
201.32296	

Note. Comparison between spectral and variational methods. The latter is provided by Ref. [12]. $\omega = 500.0$.

$^{(e)}$ 64 sample points, $\Delta t = 0.0002$, 64K time steps; $\Phi(0) = P_0(\cos\theta) + P_1(\cos\theta)$.

For $I = 1/2$ the Schrödinger equation can be written

$$i\frac{\partial \Phi}{\partial t} = -\left[\frac{\partial^2 \Phi}{\partial \theta^2} + \cot\theta \frac{\partial \Phi}{\partial \theta} - \frac{m^2}{\sin^2\theta}\Phi\right] - \omega \cos\theta \Phi, \tag{26}$$

where $\omega = pE$.

Computations were performed for $m = 0$ using an initial state consisting of linear combinations of Legendre polynomials. Energy eigenvalues calculated by the spectral method are presented in Tables IIa-IId, where they are compared with results obtained using a variational technique and perturbation theory, when applicable. The latter results are the work of von Meyenn [12]. Whenever possible the eigenvalue is designated by the l-value corresponding to the unperturbed state.

There is agreement with Ref. [12] to all five significant figures quoted in the reference in nearly every case. The eigenvalues unaccompanied by values from Ref. [12] represent additional eigenvalues determined from the input wave packets without further computational effort. Because this application was intended as an illustration, no attempt has been made to optimize with respect to either the number of grid points or the time step.

Figure 3 shows the initial and final probability distributions for $\omega = 5.0$ and for the initial wave packet composed of P_0 through P_{15}, taken with equal amplitudes.

6. Conclusion

We have demonstrated a finite Fourier series method for treating the angular derivatives in the Schrödinger equation in spherical coordinates that is accurate across the entire spectrum of the angular momentum operator. This implies that any bandlimited solution of the Schrödinger equation can be determined to high accuracy for an appropriate sampling grid and that there should be no advantage as far as accuracy is concerned to using spherical harmonics as a basis. The method should make it possible to apply the full accuracy, efficiency, and power of the finite Fourier series method to wave packet propagation in a variety of geometries and dimensions.

Acknowledgments

The authors are indebted to M. D. Feit for valuable discussion. This work was performed under the auspices of the U.S. Department of Energy by the Lawrence Livermore National Laboratory under Contract W-7405-ENG-48.

References

1. M. D. Feit, J. A. Fleck, Jr., and A. Steiger, *J. Comput. Phys.* **47**, 412 (1983).
2. M. D. Feit and J. A. Fleck, Jr., *J. Chem. Phys.* **78**, 301 (1983).
3. M. R. Hermann and J. A. Fleck, Jr., *Phys. Rev. A* **38**, 6000 (1988).
4. D. Kosloff and R. Kosloff, *J. Comput. Phys.* **52**, 35 (1983).
5. R. Kosloff and D. Kosloff, *J. Comput. Phys.* **63**, 363 (1986).
6. H. De Raedt, *Comput. Phys. Rep.* **7**, 3 (1987).
7. R. Heather and H. Metiu, *J. Chem. Phys.* **86**, 5009 (1987).
8. M. D. Feit and J. A. Fleck, Jr., *Opt. Lett.* **14**, 662 (1989).
9. A. E. Siegman, *Opt. Lett.* **1**, 13 (1977).
10. W. H. Press, B. P. Flannery, S. A. Teukolsky, and W. T. Vetterling, *Numerical Recipes* (Cambridge Univ. Press, Cambridge/New York, 1986).
11. H. Tal-Ezer and R. Kosloff, *J. Chem. Phys.* **81** (1984); see also H. Tal-Ezer, *SIAM J. Numer. Anal.* **23**, 11 (1986).
12. K. Von Meynenn, *Z. Phys.* **231**, 154 (1970).